JrnlID 248_ArtID 1069_Proof# 1 - 12/09/2017

Microb Ecol
DOI 10.1007/s00248-017-1069-9

ENVIRONMENTAL MICROBIOLOGY

The Ecology of One Cosmopolitan, One Newly Introduced and One Occasionally Advected Species from the Genus *Skeletonema* in a Highly Structured Ecosystem, the Northern Adriatic

Q1 **D. Maric Pfannkuchen[1] · J. Godrijan[2] · M. Smodlaka Tankovic[1] · A. Baricevic[1] · N. Kuzat[1] · T. Djakovac[1] · Emina Pustijanac[3] · R. Jahn[4] · M. Pfannkuchen[1]**

Received: 19 July 2017 / Accepted: 5 September 2017

Abstract The diatom genus *Skeletonema* is globally distributed and often an important constituent of the phytoplankton community. In the marine phytoplankton of the northern Adriatic Sea, we found three species of the genus *Skeletonema*: *Skeletonema menzelii, Skeletonema marinoi* and *Skeletonema grevillei*. Making use of the steep ecological gradients that characterise the northern Adriatic, along which we could observe those species, we report here on the ecological circumstances under which those species thrive and how their respective populations are globally connected. This is the first detailed ecological study for the species *S. grevillei*. This study is also the first report for *S. grevillei* for the Adriatic Sea and Mediterranean together with additional electron microscopic details on fresh in situ samples for this species. *S. marinoi* appears to clearly prefer strong freshwater influence and high nutrient concentrations delivered by low salinity waters. It can outcompete other diatom species and dominate microphytoplankton blooms. *S. grevillei* on the other hand appears to thrive in high nutrient concentrations triggered by water column mixing. It also appears to prefer higher salinity waters and coastal embayments. Genetic analysis of *S. grevillei* demonstrated a peculiar dissimilarity with isolates from coastal waters off Yemen, India, Oman and China. However, a closely related sequence was isolated from coastal waters off Japan. These results indicate that *S. grevillei* is an introduced species, possibly transported by ballast waters. *S. menzelii* is a sporadic visitor in the northern Adriatic, advected from rather oligotrophic middle Adriatic waters and never dominates the phytoplankton community in the northern Adriatic.

Keywords Phytoplankton · Northern Adriatic · Diatoms · *Skeletonema marinoi* · *Skeletonema grevillei*

Abbreviations

FP	Fultoportula
FPP	Fultoportula process
IFPP	Intercalary fultoportula process
IRP	Intercalary rimoportula
IRPP	Intercalary rimoportula process
RP	Rimoportula
RPP	Rimoportula process
TFP	Terminal fultoportula
TFPP	Terminal fultoportula process
TRP	Terminal rimoportula
TRPP	Terminal rimoportula process

Introduction

Diatoms are ecologically one of the most important phytoplankton groups, responsible for nearly one quarter of global

Electronic supplementary material The online version of this article (https://doi.org/10.1007/s00248-017-1069-9) contains supplementary material, which is available to authorized users.

✉ M. Pfannkuchen
martin.pfannkuchen@cim.irb.hr

[1] Ruđer Bošković Institute, Center for Marine Research, G. Paliaga 5, HR-52210 Rovinj, Croatia

[2] Division for Marine and Environmental Research, Ruđer Bošković Institute, Bijenička cesta 54, Zagreb, Croatia

[3] Department for Natural and Health Sciences, Juraj Dobrila University of Pula, Zagrebačka 30, HR-52100 Pula, Croatia

[4] Botanischer Garten und Botanisches Museum Berlin-Dahlem, Freie Universität Berlin, Königin-Luise-Str.6-8, Berlin, Germany

primary production and 40% of marine primary production [1]. The major diatom blooms are typical of coastal oceans and upwelling zones, in which nutrient levels are high [2]. *Skeletonema* is one of the globally most common/abundant coastal diatom genera, together with *Nitzschia*, *Achnanthes* and *Cocconeis* [3]. Species from the genus *Skeletonema* are reported to often form dense blooms [4–9].

More than 150 years have passed since the original description of the genus *Skeletonema* [10], and until the early 2000s, it was usually referred to as *Skeletonema costatum* due to the difficulty of light microscope identification [11]. In the early 2000s, more detailed morphological investigations together with new molecular insights revealed a more complex taxonomic and genetic diversity within the genus *Skeletonema* [12], and to this day, there are more than 20 different species described, which formerly were recognised as only one species [13]. Those new findings have raised the question which *Skeletonema* we are/were counting as *S. costatum*, and what are the methods for proper but effective species identification? Recently, Hevia-Orube et al. [14] recognised those questions and used molecular and microscopical techniques on three species *S. costatum*, *Skeletonema dohrnii* and *Skeletonema menzelii.* These methods are necessary for deciphering the ecology of this cryptic genus, but we are far from understanding the ecology for the whole diversity of the genus. There are currently 1450 scientific reports available containing information about *S. costatum*, 138 reports with information about *Skeletonema marinoi*, 12 reports with information on *S. menzelii* and 7 reports with information on *Skeletonema grevillei*.

Species from the genus *Skeletonema* are characterised by cylindrical cells, with long tubular processes associated with a peripheral ring of fultoportules. The tubular processes run perpendicular to the valve and link to those of sibling valves to form permanent colonies of variable length [3]. During the revision of the genus, *S. marinoi* was described and the Adriatic Sea was named as its type locality [12]. *S. marinoi* is one of the key diatom species in the Adriatic Sea. In the northern Adriatic, it regularly occurs during winter months being the major constituent of the winter-early spring bloom. But it has been found in Hong Kong and at the east coast of the USA as well. Thus, *S. marinoi* is considered a cosmopolitan species. Moreover, *S. marinoi* is generally considered to be a fast bloom-forming species in rather eutrophic conditions.

The northern Adriatic is a shallow basin and the most northern part of the Mediterranean. It is characterised by strong and dynamic ecological gradients under the governing influence of the Mediterranean's largest freshwater and nutrient input, the River Po. It is, furthermore, prone to expressed changes in water temperature due to its shallowness and strong, cold wind situations [15–18]. This wide range of conditions makes the Adriatic well suited for the study of ecological preferences of phytoplankton species. The aim of this paper is to take a closer look into the diversity and ecology of the genus *Skeletonema* in the northern Adriatic Sea and to show that the increased taxonomic resolution helps in explaining the ecological range of *Skeletonema* species in the northern Adriatic. For this, we inspected the monthly long-term phytoplankton records collected in the northern Adriatic Sea. And due to the cryptic nature of the genus, we also undertook genetic analysis and electron microscopy on isolates from the selected stations and different bloom and non-bloom events.

Materials and Methods

Study Area

All sampling stations are within the northern Adriatic (NA) (Fig. 1a). The NA is the northern most, semi-enclosed part of the Mediterranean (Fig. 1b). It is characterised by strong gradients of nutrient concentrations, and its plankton can be generally considered to be phosphate limited. However, the Mediterranean's largest freshwater input, the River Po, is a strong nutrient source for the area [17, 19, 20]. The study area is generally shallow with maximum depths of 45–60 m.

Sampling

As part of a Croatian long-term monitoring program of phytoplankton assemblages in the northern Adriatic Sea [21], water and net samples were collected monthly at 17 stations across the northern Adriatic through the period 1998–2009. Additional 15 stations were sampled during 2014 and 2015 in Lim Chanel, Pula Harbour, Rijeka Harbour and Kvarner Bay (Fig. 1). Water and phytoplankton samples were taken at the water surface, in 5, 10, 15 and 20 m depth, as well as 1 m above the seafloor. Overall, 9599 samples were analysed. In 1718 samples, we found *Skeletonema* species.

Conductivity–temperature–depth (CTD) profiles were recorded with an SBE 25 Sealogger CTD probe (Sea-Bird Electronics, Inc., Bellevue, Washington, USA) including oxygen saturation.

Sample Analysis

The following nutrients: nitrate (NO_3), nitrite (NO_2), orthophosphate (PO_4) and orthosilicate (SiO_4) were measured by spectrophotometric methods [22]. Ammonium (NH_4) was analysed by a modified technique of the indophenol method [23]. Measurements were performed on a Shimadzu UV-Mini 1240 spectrophotometer with 10 cm cells. In statistical analyses, total inorganic nitrogen (TIN, sum of NO_3, NO_2 and NH_4) was used. A 500-mL subsample for the determination of chlorophyll *a* was filtered onto Whatman GF/C filters and

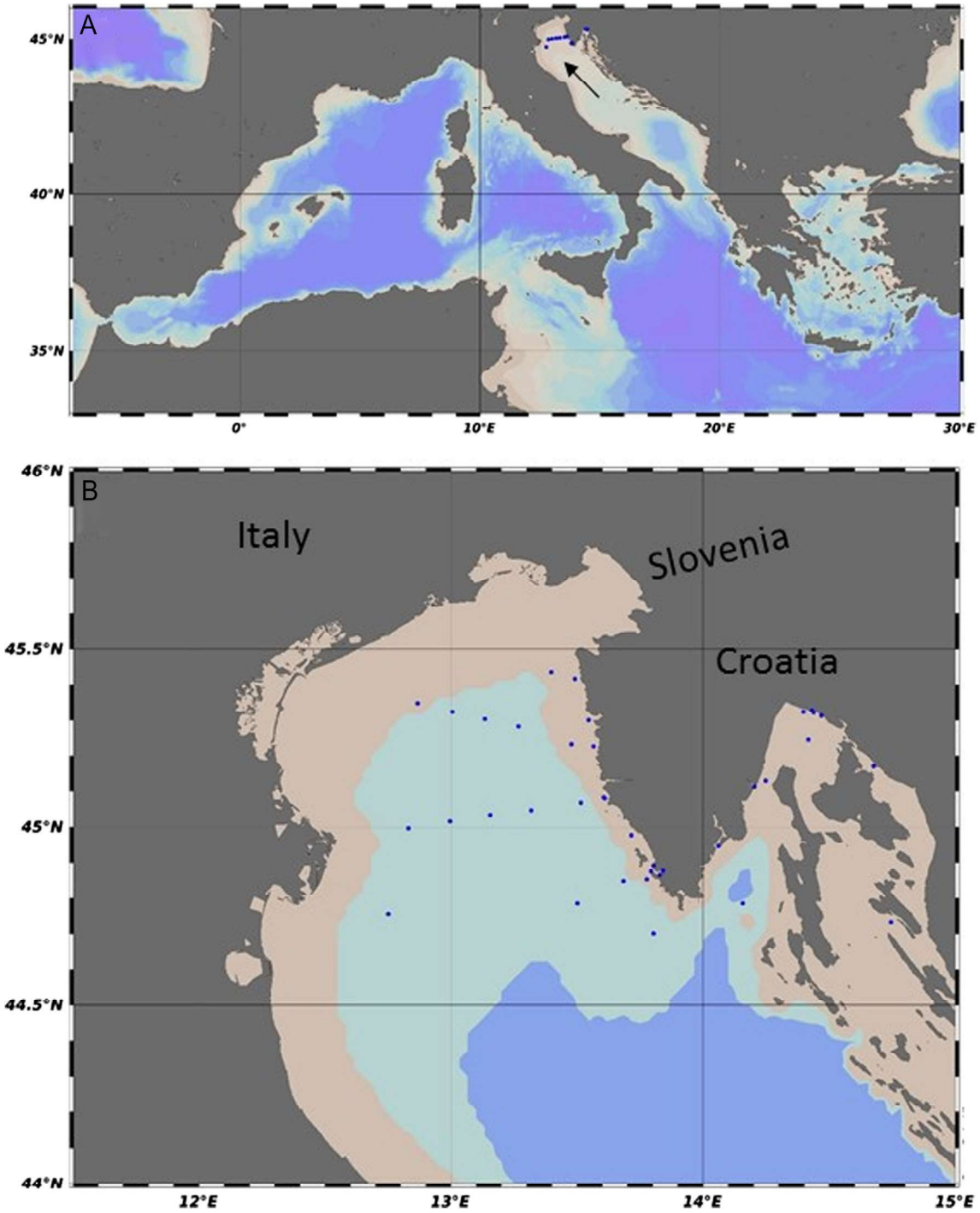

Fig. 1 **a** Location of the Northern Adriatic in the Mediterranean (*arrow*). **b** Map of the northern Adriatic with the sampling stations

immediately frozen at − 20 °C until analysis (within a week). Total chlorophyll *a* concentrations were determined on a Turner TD-700 fluorimeter [22] after 3 h of extraction in 90% acetone (in the dark, with grinding). Further details were described earlier [24].

Phytoplankton samples, 200 mL, were fixed with neutralised formaldehyde (2% final concentration). Phytoplankton cells were counted in 50 mL subsamples after 40 h of sedimentation time [25], using an Axiovert 200 microscope (Zeiss GmbH, Oberkochen, Germany) and following the Utermöhl [26] method. Prior to the description of *S. marinoi* in 2005, *S. marinoi* was identified as *S. costatum* in our dataset. However, genetic and electron microscopical analysis on samples from 2006 demonstrated that the taxon named *S. costatum* in our analyses prior to the description of *S. marinoi,* in fact had to be attributed to the taxon *S. marinoi*.

S. costatum as delineated by Zingone et al. [27] was never observed during ultrastructural analyses of our samples from the NA. For the here-reported analyses, we attributed all abundances recorded for the taxon *S. costatum* prior to 2005 to the taxon *S. marinoi*. Overall, 9599 samples were analysed. In 1718 samples, we found *Skeletonema* species.

Colonies of the *Skeletonema* species were manually isolated with a micropipette from live net samples collected at various stations in the northern Adriatic Sea. Colonial cells were grown into monoclonal batch cultures in 100 mL f/2 medium [28] and incubated at 18 °C and 75 µmol photons m^{-2} s^{-1} on 12:12 h light/dark photoperiod.

Net sample material and cultures were acid cleaned of organic matter for electron microscopy.

For EM preparation, samples were treated with acids (1:1:4, sample:HNO_3:H_2SO_4), boiled for a few minutes and then washed with distilled water three times. Frustules were allowed to sink for a few minutes between washing steps. For transmission electron microscopical (TEM) examination, a drop of cleaned material was mounted on a 100-mesh copper grid covered with pioloform (Agar Scientific Ltd., Stansted, UK), air dried and observed with an FEI Tecnai TEM (FEI Co., Eindhoven, The Netherlands). For scanning electron microscopical (SEM) examination, the cleaned diatom material was dropped on silica waver or directly on aluminium object carriers. The object carriers were air dried and examined without sputter coating. When needed, samples were gold coated with a sputter coater (S150A Sputter coater; Edwards Ltd., Crawley, UK) and observed with a Philips 515 SEM (FEI Co.).

Morphological features were observed in LM, TEM and SEM. Ultrastructural morphometric data were obtained in TEM and SEM. All LM observations were carried out on field samples and monoclonal cultures (in exponential phase) using a Zeiss Axiovert 200 microscope (Carl Zeiss, Oberkochen, Germany) equipped with Nomarski differential interference contrast (DIC), phase contrast and bright-field optics. Light micrographs were taken using a Zeiss Axiocam digital camera. The terminology used to describe ultrastructural features of *Skeletonema* species follows Anonymous [29], Ross et al. [30] and the original descriptions in Sarno [12] and Zingone et al. [27].

DNA Extraction, PCR Amplification and Sequencing

For molecular analysis, monoclonal cultures of *Skeletonema* species were harvested by centrifugation at 5000 rpm for 5 min (5417R, rotor F453011; Eppendorf AG, Hamburg, Germany). DNA was isolated with the DNA Plant Mini Kit (Qiagen GmbH, Hilden, Germany) according to the producer's recommendations. The hypervariable V4 region of the 18S ribosomal RNA (rRNA) gene was amplified using the primers 5-ATTCCAGCTCCAATAGCG-3 and 5-GACTACGATGGTATCTAATC-3 according to Zimmermann et al. [31] and sequenced (using the same primers) on an ABI PRISM 3100 Avant Genetic Analyser (Applied Biosystems, Foster City, CA, USA) according to the company's recommendations. The D1–D3 region of the 28S rRNA gene was amplified using the primers 5-ACCCGCTGAATTTAAGCATA-3 and 5-ACGAACGATTTGCACGTCAG-3 and sequenced as described above [32]. The resulting sequences from two runs for each direction were compared to exclude sequencing mistakes by majority rule (3:1).

Genetic Marker Analysis

The resulting sequences were aligned into an alignment of near full-length 18S and 28S rDNA genes. The alignments were based on the alignment of all publicly available full-length 18S and 28S rRNA gene sequences, including more than 1200 diatom sequences (SSURef_98_Silva_20_03_09_opt database and LSURef_98_Silva_20_03_09_opt) [33]. Sequences were manually aligned and compared using the ARB 5.1 software package [34] following the protocol suggested by Peplies et al., specifically using the neighbour-joining algorhythm included in the Arb software package [35]. The alignment for the 18S rDNA includes 437 positions, while the alignment for the 28S rDNA fragment includes 680 positions. Genetic distances were calculated as percentages.

Statistical Analysis

Statistical analysis as well as graphical presentation of the results was performed using the software package R and included core packages as well as programs from the packages Hmisc, base and ggplot2 [36–39]. In box-and-whisker plots, the top and the bottom of the boxes represent the 25th and 75th percentiles, respectively. The centre line delineates the 50th percentile. Outliers are shown as dots and where defined as either greater than the 3rd quantile + 1.5 × (quantile 3 − quantile 1) or smaller than quantile 1 − 1.5 × (quantile 3 − quantile 1). Whiskers (notches) extend to the most extreme data point that is less than 1.5 times the box size away from the box. Correlation graphs were produced using the package PerformanceAnalytics [40]. In the correlation graphs, results were grouped according to their P value in three groups: $P < 0.001$, $P < 0.01$ and $P < 0.05$, following the discussion by Fisher [41]. In the reported cases, correlations with a P value smaller than 0.05 where considered significant.

Results

Taxonomy and Morphometrics of *Skeletonema* spp. in the Northern Adriatic.

All three detected species, *S. marinoi, S. grevillei* and *S. menzelii,* were inspected microscopically. The morphology of the observed *S. marinoi* fits and falls within the details and ranges described earlier [12, 27]. Cells formed long curved or coiled chains. Valve diameter varied from 2 to 12 μm. Ultrastructural details observed in *S. marinoi* during this survey are presented in Supplementary Fig. 1. External processes of the fultoportulae were open, with flat and flared tips and jagged distal margins. Each process connected with one or two processes of the sibling valve. The rimoportula was close to the valve face margin in intercalary valves and subcentral in terminal valves. External process of the rimoportula was short in intercalary valves, long in terminal valves of the colony. Copulae with transverse ribs were interspaced by rows of pores. The valve face was slightly convex; the mantle was vertical. The fultoportula processes (FPPs) were open along their entire length. Their distal end was flattened and flared, with a dentate margin. The intercalary fultoportula process (IFPPs) of sibling valves were either aligned, with a 1:1 linkage, or displaced, with a 1:2 linkages and a zigzag connection line. The interlocking between IFPPs was in all cases a plain joint, with no intricate knots or knuckles. The flared tips of the IFPPs overlapped with edges that interdigitated with one another. The TRP was located close to the central annulus or midway between the centre and the margin of the valve and had a long tubular process with a slightly flared or trumpet-or cup-shaped apex. The IRP was short and at the edge of the valve face. The copulae showed the typical central ridge, which was flanked on both sides by transverse ribs interspaced by rows of pores.

For *S. grevillei*, a detailed electron microscopic analysis revealed new characteristics of the species. In the original description of *S. grevillei* based on the type material, the authors state that in light micrographs, cells have a delicate aspect, with the cingulum often collapsed [27]. In our samples, the cingulum in LM was intact (see Fig. 2a for a SEM aspect of the cingulum). We observed colonies with 3–28 cells in both monoclonal cultures and in situ samples. In our results, the valve face was slightly convex and the pervalvar axis was generally longer than or as long as the cell diameter like in the original description as well [12, 27, 42]. In our results, the cell diameter was from 5 to 19 μm, which extends the measurements from original descriptions 6–12 (Table 1). The IFPPs were rather long (8.5 ± 1.6 μm, n = 33 against 6.7 ± 1.6 μm, n = 35), each joining one IFPP of the adjacent cells (1:1 junction), with a thickening at the joint (Fig. 2a–f). Only rarely one IFPP joined two IFPPs of the next valve (1:2 junction) (not shown). A zigzag line at the level of the connection was never observed which is in accordance with the original description [27].

The length of the observed TFPPs was 5.6 ± 1.8 μm (n = 10), which is very close to the original description, and they are visibly thickened at their tips (Fig. 2a, b). A transverse ridge forms a straight line across the bases of the processes, and other ridges are visible on the valve mantle (Fig. 2a and d). With EM, the mantle ridges are seen as a scalloped edging of ridges at the base of the FPPs (Fig. 2a–d, f–h). The straight line visible in LM corresponds to a series of silica ridges with concave rims that connect the internal faces of the bases of the FPPs [27]. A second and at times a third series of ridges, more or less parallel to the first one, may join the lateral bases of the FPPs (Fig. 2f–h). Finally, two opposite concave ridges at the external base of each FPP delimit a circular or oval hole (Fig. 2a–e). These structures were more or less developed in different individuals. Those findings are in accordance to Naik [43] who also observed larger silica ridges compared with the original description.

The valve face showed a central annulus. Its solid area was interspaced with an irregular agglomeration of small, round pores. Radial, bifurcating and delicate ribs covered the valve face and were separated by small, round pores. On the valve margin, delicate ribs connected the radial, delicate ribs perpendicular to those. Thus rectangular areas were formed between the delicate ribs, which were entirely filled with small, round pores (Fig. 2c, h).

The FPPs open along their entire length (Fig. 2a–h), and the distance between them was 1.5–2.5 μm. The fultoportulae processes in the terminal valve extremities were irregularly truncated and pointed at their lateral ends (Fig. 2a); we observed generally one small spine. The interlocking between IFPPs was particularly intricate and tight, resembling a bone knuckle (Fig. 2d, f), same as documented in the original description of the species. The TRP was located just inside the marginal ring of TFPs (Fig. 2b) and bore a long tubular process (6.1 ± 1.8 μm, n = 5) even longer than in original description, which was wider and obliquely truncated at its top, with a tubular end (Fig. 2b). The intercalary RP was located marginally and had a short (0.6 μm) and tubular external process (Fig. 2e) similar as described before. We also found incidents where the IRP was entirely incorporated in the rather massive silica ridge between IFPP. Such IRP was not described before. Sometimes, it was incorporated in silica ridges and was very difficult to spot and measure. A ridge went medially along the whole length of the copula (Fig. 2k). Thin transversal ribs, generally bifurcate at their ends and interspaced with a hyaline

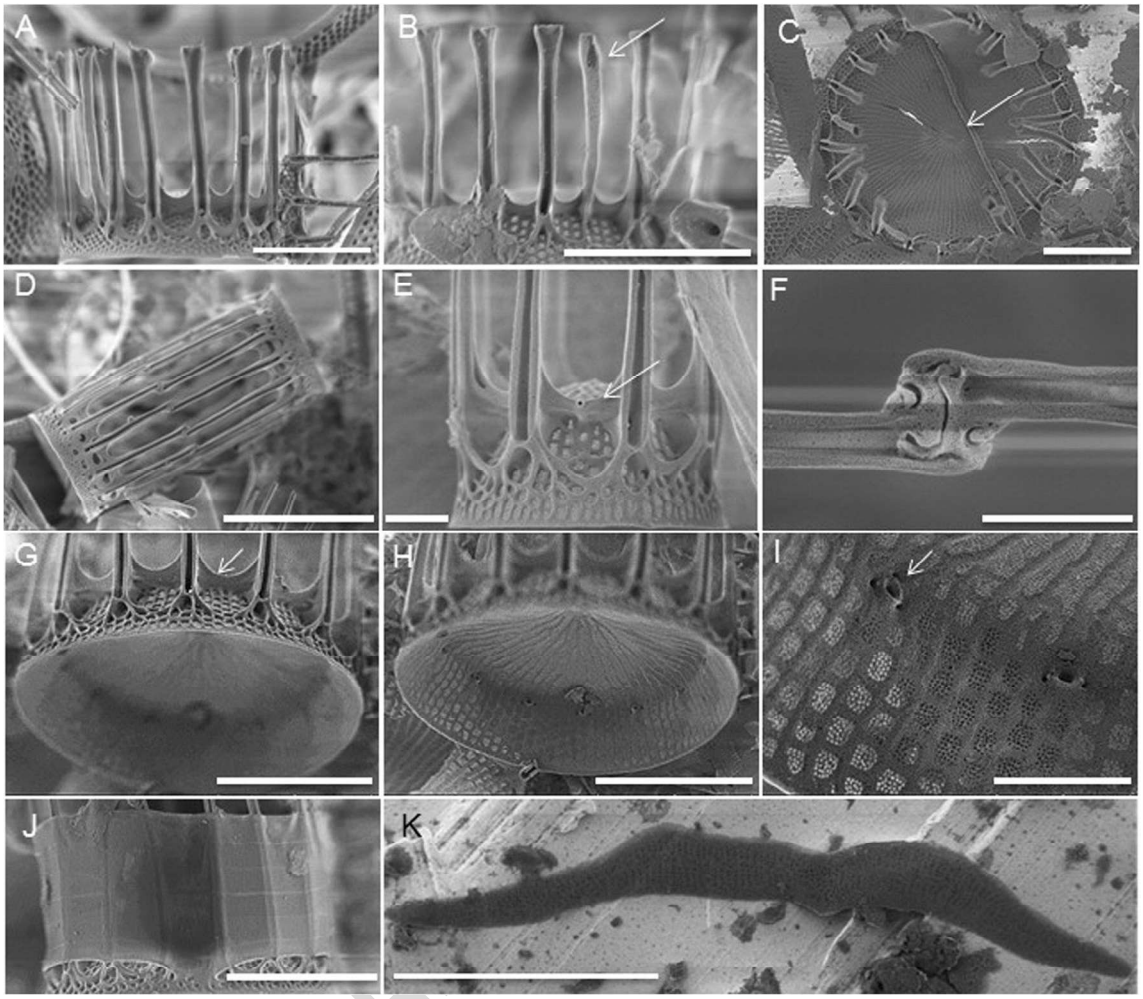

Fig. 2 SEM micrographs of *S. grevillei* from field samples. **a** Terminal valve of a colony. Distal ends of the TFPPs with one small spine. *Scale bar*, 5 μm. **b** Terminal valve of the colony with the long marginal TRPP (*arrow*) with its obliquely truncated margin. *Scale bar*, 5 μm. **c** Terminal valve in valve view with the TRP, the annulus (*arrow*), the TFPs and the TFPPs. *Scale bar*, 5 μm. **d** Intercalary valve with the knuckle junctions 1:1. *Scale bar*, 10 μm. **e** Intercalary valve with ridges between IFPP bases and a small IRPP (*arrow*). *Scale bar*, 1 μm. **f** Detail of knuckle-like junction. *Scale bar*, 1 μm. **g** Detail of an intercalary valve with several series of silica ridges (*arrows*) joining the IFPP bases. *Scale bar*, 4 μm. **h** Detail of an intercalary valve from inner view showing joining the FP bases. *Scale bar*, 4 μm. **i** Internal view of intercalary valve detail showing a FP with three satellite pores (*arrows*). *Scale bar*, 1 μm. **j** Cingular bands with the trasversal ribs interspaced with hyaline areas placed on valve. *Scale bar*, 5 μm. **k** Single cingular band with the trasversal ribs. *Scale bar*, 5 μm

area were observed. A comparison between the here-reported values and the original description of *S. grevillei* is presented in Table 1.

For *S. menzelli*, no cultures were isolated and no electron microscopical analysis was performed for the species. The observed cells from in situ samples however showed no apparent divergence from the original morphological descriptions and recent reports [44, 45]. We observed single cells and chains of two cells, and longer chains were never observed. The FPs were located marginally near the transition from the valve face to the mantle. Ultrastructural traits like the missing costae and areolae as well as the two satellite pores (as opposed to three in other Skeletonema species) were not analysed [12].

Ecology

Figure 3 shows a box-and-whisker plot of all abundances of *S. marinoi* observed between 1999 and 2016 on a transect across the northern Adriatic (black). It demonstrates that *S. marinoi* was a regular component of the northern Adriatic phytoplankton community with an expressed winter-early spring bloom.

There was an irregularly occurring late summer bloom of *Skeletonema* sp. (July–September) (Fig. 3), assigned to *S. marinoi*; however, it was never extensively characterised via electron microscopy or using molecular markers and hence it cannot be excluded that also *S. grevillei* is found during such blooms.

Q2 t1.1 **Table 1** Main morphometric data of *Skeletonema marinoi* and *Skeletonema grevillei* from this study compared with the original description from Zingone et al. [27] and Sarno et al. [12]

t1.2		*S. marinoi* (this study)			Sarno et al. [12]			*S. grevillei* (this study)			Zingone et al. [27]		
t1.3		Min-max	Average ± SD	*n*	Min-max	Average ± SD	*n*	Min-max	Average ± SD	*n*	Min-max	Average ± SD	*n*
t1.4	Cell diameter (μm)	5–12	8.95 ± 1.76	39	2–12	4.3 ± 1.9	300	*5–19*	11.1 ± 2.7	24	6–12	7.4 ± 2.2	20
t1.5	Distance between cells (μm)	6.33–10.4	8 ± 1.4	12	0.5–1.5	0.9 ± 0.2	26	9.3–*23*	16.9 ± 4.9	9	8–20	13.4 ± 3.2	17
t1.6	Cells per colony	3–20	8.5 ± 7.7	40	2–45	16.2 ± 10.9	125	3–28	13.9 ± 7.4	30	3–8	3.8 ± 1.9	13
t1.7	FPPs in 10 μm	8–*12*			9–11	10 ± 1	5	6–9	7.2 ± 0.9	11	7–12	8.2 ± 1.4	13
t1.8	Distance between FPPs (μm)	0.9–*1.8*	1.4 ± 0.3	15	0.5–1.5	0.9 ± 0.2	26	1.4–*2.5*	*2.0* ± 0.24	22	0.7–1.5	1 ± 0.2	9

Values set in italics exceed ranges from the original descriptions

S. grevillei Sarno and Zingone was observed for the first time in the Adriatic Sea during the autumn bloom 2014 when it reached high abundances. This is simultaneously the first record of *S. grevillei* in the Mediterranean. Figure 3 shows a box-and-whisker plot for abundances of *S. grevillei* when observed between the years 2014 and 2016 (grey).

The highest abundance was 2.5×10^5 cells L^{-1}. *S. grevillei* appeared in September with peak abundances in November/December and lasted until January/February.

S. menzelii was found only sporadically and in very low abundances across the entire study area.

Figures 4 and 5 show the geographical distribution of abundances for *S. marinoi* (Fig. 4) and *S. grevillei* (Fig. 5) in the study area. We found highest abundances for *S. marinoi* near the western Adriatic coast in waters close to the mouth of the River Po, while highest abundances for *S. grevillei* were observed in the harbours on the eastern Adriatic coast. The highest abundances were found in the surface layer from 0 to 10 m depth in Rijeka Harbour (Fig. 5).

Figure 6 shows box-and-whisker plots for environmental parameter recorded when *S. marinoi* or *S. grevillei* respectively were found in the samples. A significant difference was

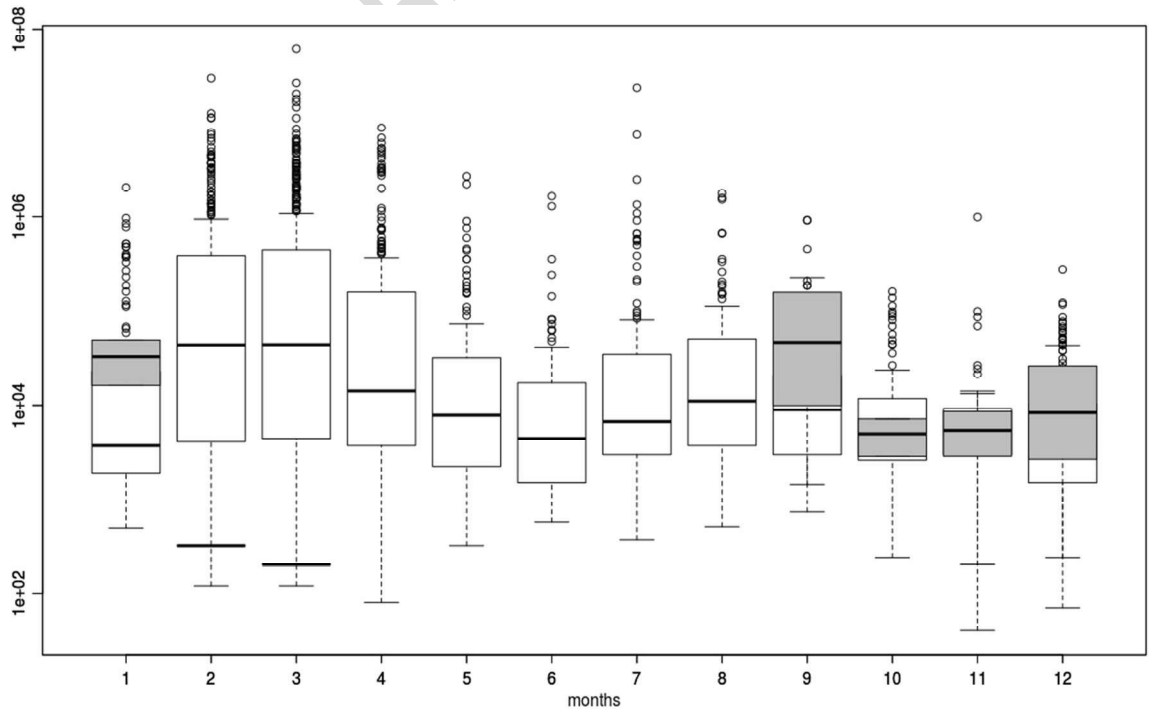

Fig. 3 Box-and-whisker plot of recorded abundances for *S. marinoi* (*open boxes*) between 1999 and 2016 as well as for *S. grevillei* (*grey*) between 2014 and 2016. Observations are grouped by month of observations

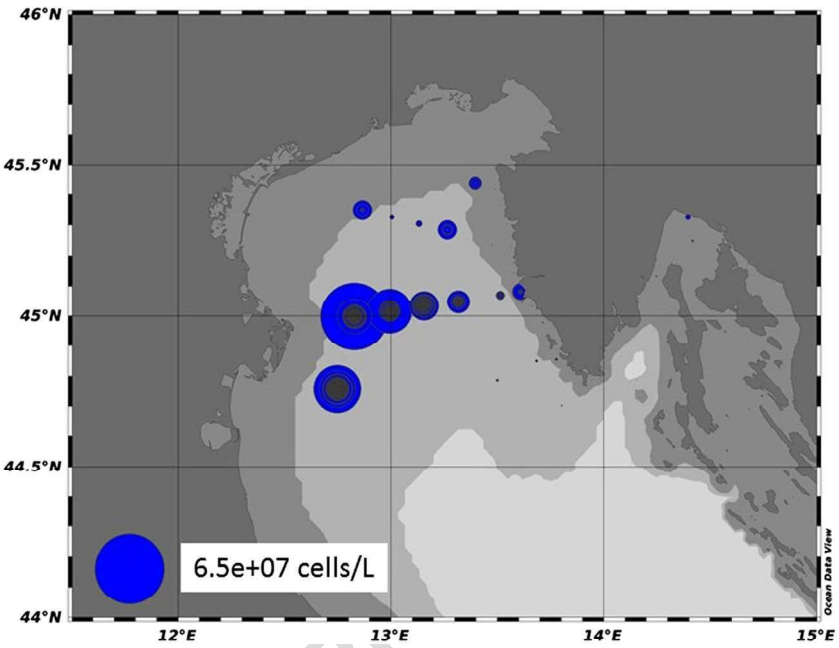

Fig. 4 Spatial distribution of observed abundances of *S. marinoi* between 1999 and 2016

observed in the oxygen saturation values accompanying *S. marinoi* and *S. grevillei*. A two-sample *t* test showed the two sets of oxygen saturation values to be significantly different (*P* value < 2.2E−16). Figure 7 shows a scatter plot of oxygen saturation values and abundances for *S. marinoi* and *S. grevillei*. For all other oxygen unrelated parameters, we found rather overlapping ranges for both species. Table 2 reports descriptive statistics for both species and for all analysed parameters.

Table 3 shows the correlations between group abundances of total microphytoplankton, diatoms, dinoflagellates and coccolithophorids during occurrences of *S. marinoi* and *S. grevillei*, respectively. High correlation coefficients of 0.9 between *S. marinoi* and microphytoplankton as well as diatom

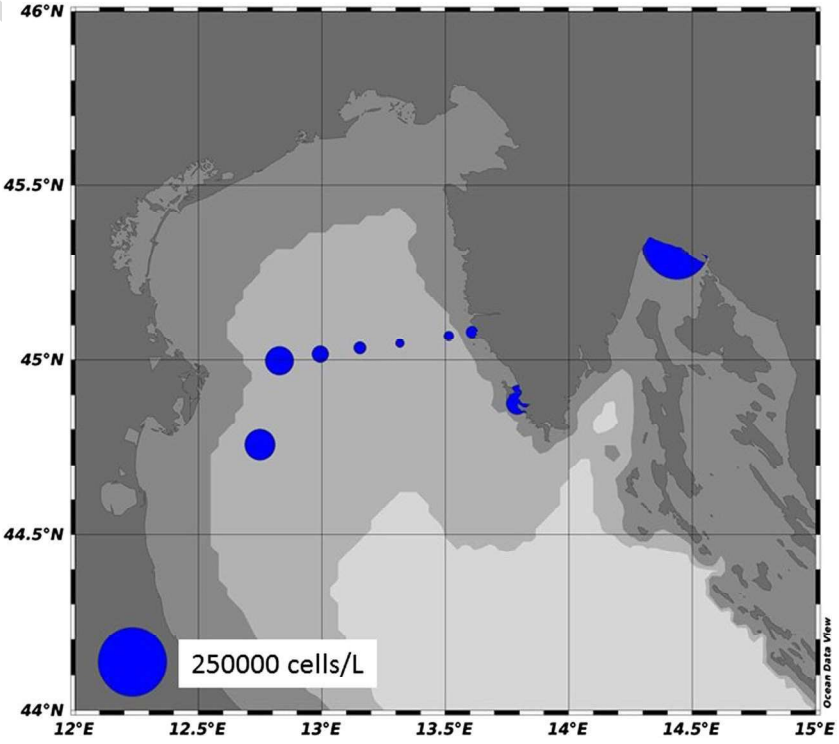

Fig. 5 Spatial distribution of observed abundances of *S. grevillei* between 2014 and 2016

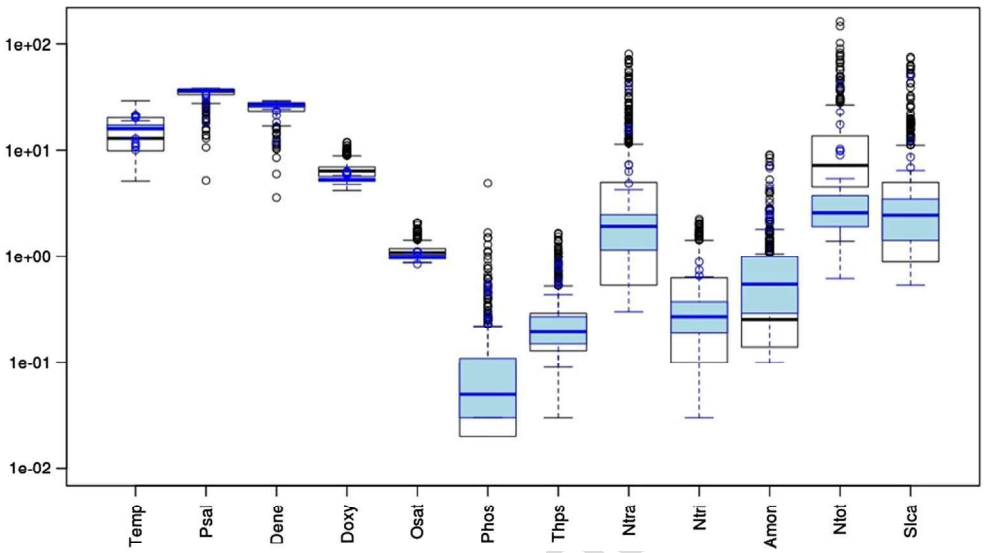

Fig. 6 Temperature, salinity, oxygen saturation and nutrient salt concentrations recorded in samples when *S. marinoi* (*black*) and *S. grevillei* (*blue*) were observed, respectively. *Temp* temperature (°C), *Psal* practical salinity, *Dene* density anomaly (kg m^{-3}), *Doxy* dissolved oxygen (mg L^{-1}), *Osat* oxygen saturation (0–1), *Phos* dissolved phosphate (µM), *Thps* total dissolved phosphor (µM), *Ntra* nitrate (µM), *Ntri* nitrite (µM), *Amon* ammonia (µM), *Ntot* total dissolved N (µM), *Slca* silica (µM)

abundances demonstrate *S. marinoi*-dominating diatom blooms. *S. grevillei* however never dominates the microphytoplankton community. Supplementary Fig. 2 gives a graphical representation of the correlations for *S. marinoi* (a) and *S. grevillei* (b) summarised in Table 3.

Genetic Analysis

We analysed the hypervariable V4 Region of the SSU rDNA as well as the D1–D3 region of the LSU rDNA.

The V4 region of the SSU rDNA of *S. marinoi* from our samples (GenBank accession number MF772522) was found to be identical to the available sequences published earlier from the western coast of the Adriatic sea (NCBI accession numbers AJ632213, EF433521, AF462060, AJ632212, AJ632216, AJ632214, EF138932, EF138940, EF138939, EF433519, EF138934, HM236346, HM236347, JF489952, JF489958, HM236345, HM236349, HM236348, JF489953, KJ671706, KJ671705, KJ671707, KT860966 and KJ671708) as well as to sequences published from isolates from the western Mediterranean (KR091067) and the Baltic Sea (HH805045).

The D1–D3 region of the LSU rDNA of *S. marinoi* from our samples (GenBank accession number MF772714) was found to be identical to the available sequences published earlier from Hong Kong Bay (AJ633529) and from the

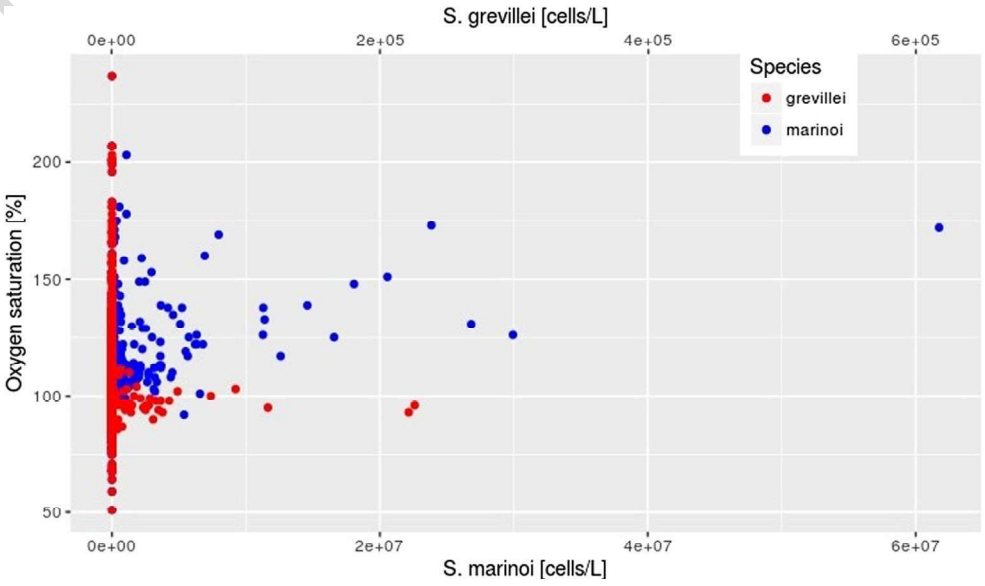

Fig. 7 Oxygen saturations recorded in samples when *S. marinoi* (*blue*) and *S. grevillei* (*red*) were observed, respectively

JmlID 248_ArtID 1069_Proof# 1 - 12/09/2017

t2.1 **Table 2** Environmental parameters found in samples, when *Skeletonema marinoi* or *Skeletonema grevillei* were present

		Temp (°C)	PSU	Density anomaly (kg m^{-3})	Dissolved oxygen (mg L^{-1})	Oxygen saturation	P (μM)	Total P (μM)	Nitrate (μM)	Nitrite (μM)	Ammonia (μM)	Total N (μM)	Silica (μM)
t2.3	*S. marinoi*												
t2.4	Mean	15.14	34.91	25.72	6.52	1.14	0.11	0.26	5.42	0.43	0.52	12.54	5.18
t2.5	SD	6.13	4.27	3.85	1.16	0.17	0.27	0.25	10.72	0.43	0.99	17.10	9.69
t2.6	Median	13.00	36.34	26.74	6.39	1.09	0.05	0.18	1.57	0.28	0.26	7.22	2.30
t2.7	Min	5.15	5.21	3.58	4.17	0.87	0.00	0.03	0.00	0.00	0.00	1.39	0.00
t2.8	Max	29.70	38.54	29.88	11.98	2.09	4.90	1.64	80.67	2.27	9.04	163.50	75.70
t2.9	*S. grevillei*												
t2.10	Mean	16.29	36.34	26.68	5.35	0.97	0.10	0.25	3.20	0.30	0.90	4.40	3.64
t2.11	SD	2.63	3.34	2.60	0.35	0.60	0.12	0.17	5.70	0.19	1.14	6.29	6.67
t2.12	Median	16.08	37.35	27.54	5.27	0.97	0.05	0.20	1.90	0.27	0.55	2.59	2.47
t2.13	Min	10.06	18.51	12.05	4.77	0.84	0.03	0.09	0.30	0.03	0.10	0.62	0.54
t2.14	Max	21.79	38.21	29.00	6.35	1.11	0.54	0.88	39.91	0.88	6.83	41.58	50.87

476 western coast of the Adriatic Sea (NCBI accession numbers
477 AJ633533, AJ633536, AJ633532, AJ633535, AJ633530,
478 AJ633531, AJ633534, Q396506, EF433522, EF655656,
479 FR823443, FR823447, EF433524 and FR823444).
480 Supplementary Fig. 3 shows a tree representation of
481 neighbour-joining analysis of all available sequences for the
482 V4 region of the SSU rDNA (a) and the D1–D3 region of the
483 LSU rDNA (b) of *S. grevillei*. The results clearly demonstrate
484 that for both regions, the strains isolated from the northern
485 Adriatic represent a genotype different from those found else-
486 where (SSU GenBank accession number MF772521, LSU
487 GenBank accession number MF772715). Figure 8 shows the
488 genetic distance of *S. grevillei* isolates from various areas if
489 compared with the northern Adriatic isolate. Close relatives
490 are reported from Yemen and Japan.

Discussion

491

Taxonomy and Morphometrics of *Skeletonema* spp. in the Northern Adriatic

492
493

Morphological characteristics of *S. marinoi* were found to be
494 within the ranges so far described for the species. This allows
495 us to assume that the ecological conditions found in the north-
496 ern Adriatic do not invoke dramatic morphological responses,
497 altering its silica structures from the details laid out in its
498 species descriptions [12, 46]. For *S. grevillei* however, we
499 found morphological characteristics that are either newly ob-
500 served or are slight aberrations from the original description.
501 We uncovered that *S. grevillei* is capable of forming rather
502 long chains (in situ and in cultures), which were not found
503

t3.1 **Table 3** Correlations between microphytoplankton groups and *Skeletonema marinoi* and *Skeletonema grevillei*, respectively

		Microphytoplankton		*Bacillariophyceae*		*Dinophyceae*		*Coccolithophoridae*	
t3.3		Correlation value	*P* value	Correlation value	*P* value	Correlation value	*P* value	Correlation value	*P* value
t3.4	*S. marinoi* (n = 1650)	0.90	$< 10^{-8}$	0.90	$< 10^{-8}$	0.05	0.02	0.01	0.58
t3.5	*S. grevillei* (n = 1650)	0.03	0.80	0.03	0.80	−0.12	0.35	−0.05	0.66
t3.6	*Microphytoplankton* (n = 1650)			1.00	$< 10^{-8}$	0.30	$< 10^{-8}$	0.13	1.49E−07
t3.7	*Bacillariophyceae* (n = 1650)	1.00	$< 10^{-8}$			0.29	$< 10^{-8}$	0.12	3.01E−07
t3.8	*Dinophyceae* (n = 1650)	0.30	$< 10^{-8}$	0.29	$< 10^{-8}$			0.12	8.40E−07
t3.9	*Coccolithophoridae* (n = 1650)	0.13	1.49E−07	0.12	3.01E−07	0.12	8.40E−07		

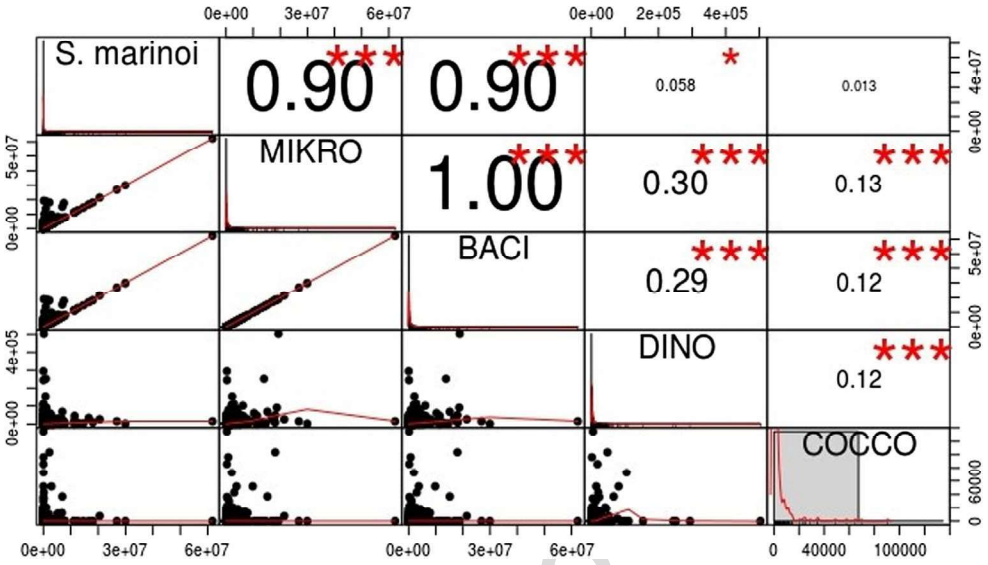

Fig. 8 Representation of genetic distances (and origin) between different isolates of *S. grevillei* and the conspecific isolates from the northern Adriatic (location marked by an *arrow*). Size and colour of the *dots* correlate to percent sequence difference in the D1–D3 region of the LSU rDNA. The *arrowhead* indicates the presentation of the sample from Yemen

in the type material nor earlier described. We extended the range for cell diameters to 5–19 μm. We can also report larger values for IFPP length (8.5 ± 1.6 μm). Contradicting the original description, we found that the valve face shows a central annulus. Its solid area is interspaced with an irregular agglomeration of small, round pores. Radial, bifurcating and delicate ribs cover the valve face and are separated by small, round pores. On the valve margin, delicate ribs connect the radial, delicate ribs perpendicular to those. Thus, rectangular areas are formed between the delicate ribs, which are entirely filled with small, round pores (Fig. 2c, h). These incidentally also represent a combination of features described for other *Skeletonema* species, which either show bifurcating radial ribs or rectangular areas only. The original description mentions that on the valve face, radial rows of rectangular areolae branch off from the central annulus. However, no EM micrograph was shown to support this statement. Our findings differ from the original description in irregular agglomeration of pores in the central annulus and more importantly in the observation that the valve face is not ornamented with rectangular areolae. For the FPP length we report again larger values (1.5–2-5 μm as opposed to 0.7–1.5 μm) than the original description. Incidentally, we found cells, where the IRP is entirely incorporated in the rather massive silica ridge between IFPP. Such IRP was not described before.

Owing to the overall similarity of the characteristics to those attributed to *S. grevillei* and the age of the type material, we nevertheless still assume that we here show *S. grevillei* (Fig. 2). This would indicate that in some instances, we might have observed morphological reactions to the ecological

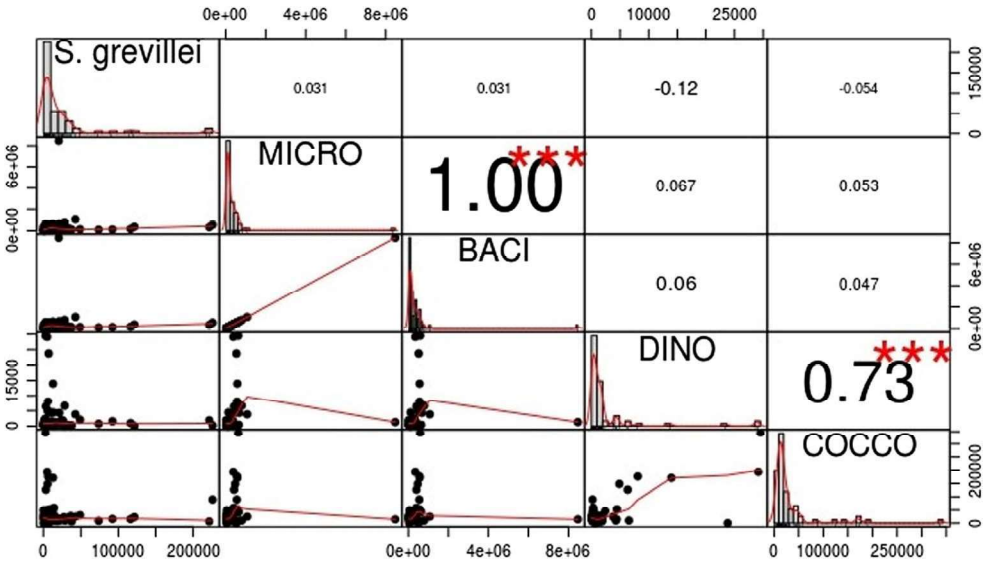

Fig. 9 High and significant correlation between *S. marinoi* abundances and total microphytoplankton as well as diatom abundances in samples containing *S. marinoi*

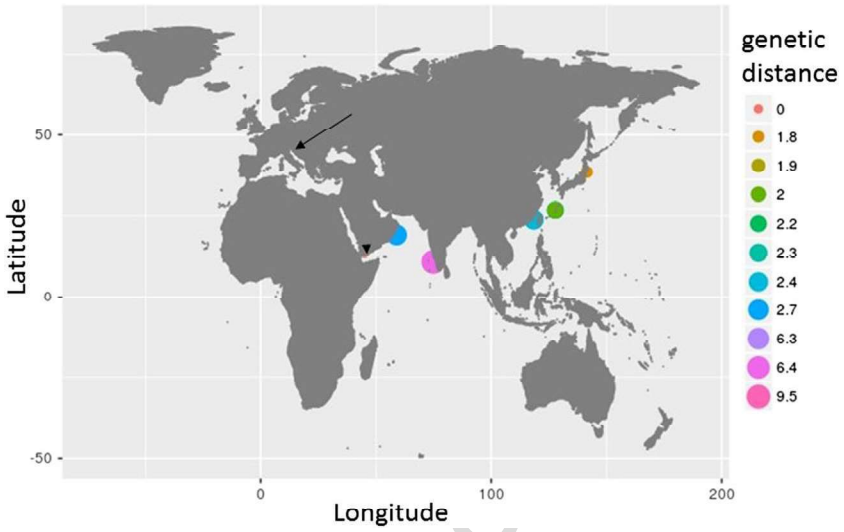

Fig. 10 Irregularly occurring late summer bloom of *Skeletonema* sp. (July–September)

conditions found in the northern Adriatic. However, we think that we added substantial information to the morphological characterisation of *S. grevillei*.

Ecology

The distribution of *Skeletonema* species identified in Sarno et al. [12] provides, in some cases, evidence of distinct ecological characteristics. The four *Skeletonema* species found in the Gulf of Naples tend to occupy different seasonal niches: *S. dohrnii* has only been found in winter, *S. pseudocostatum* blooms in late spring and early summer, *S. tropicum* is recorded in late summer and early autumn and *S. menzelii* is typical of autumn. These periods are characterised by markedly different conditions in terms of temperature (13–30 °C), salinity (25–38 psu), water column stability, photoperiod and nutrient concentrations [47]. In the northern Adriatic, we recorded three different *Skeletonema* species: *S. marinoi*, *S. grevillei* and *S. menzelii*.

In the northern Adriatic, *S. marinoi* can be found frequently from February to April and less frequently during summer. It is a regular component of the northern Adriatic winter-early spring bloom (Fig. 3). Favourable conditions for *S. marinoi* are a strong influence of nutrients mostly from the River Po. It is fast growing and outcompeting other diatom species during the bloom. Often highest abundances are found in the western part of the Northern Adriatic, where nutrient concentrations are highest (Fig. 4). It appears to thrive best in open waters under the direct influence of strong freshwater and nutrient input (Fig. 6). This explains the geographical distribution with markedly higher abundances near the River Po outflow, where salinity is lower and nutrients are delivered in high concentrations [17]. This notion is also corroborated by the rather high concentration of total nitrogen concentrations in water samples where *S. marinoi* was present in high abundances. The oxygen oversaturation in the upper layer of the water column indicates the riverine freshwater influence, as well as highly productive conditions (Fig. 7). The high and significant correlation between *S. marinoi* abundances and total microphytoplankton as well as diatom abundances in samples containing *S. marinoi* allows the conclusion that if conditions are favourable, *S. marinoi* will outcompete other diatoms and dominate a diatom bloom (Fig. 9). There is an irregularly occurring late summer bloom of *Skeletonema* sp. (July–September) (Fig. 3) which is currently assigned to *S. marinoi*; however, it was never extensively characterised via electron microscopy or molecular markers, and hence it cannot be excluded that also *S. grevillei* is found during such blooms (Fig. 10).

Our dataset contains abundance data for *S. marinoi* from before the description of *S. grevillei* [27] when most certainly observations of *S. grevillei* were reported under the species name *S. marinoi* (Fig. 3). Since the description of *S. grevillei* as a new species, it was counted as a separate species. Since then, *S. grevillei* was observed from September to January, while *S. marinoi* appears from February to August. Only rarely both species are observed simultaneously, and if so, with opposite trends in abundances. Oxygen saturation during *S. grevillei* blooms was observed to be significantly lower than during *S. marinoi* blooms, which indicates lower primary production rates as well as possibly higher respiration rates.

S. grevillei was observed for the first time (reported here) in 2014 during an autumn bloom (September–December) along the eastern Adriatic coast reaching relatively high abundances (2.6×10^5 cell L^{-1}). Before that, *S. grevillei* was only found in Hong Kong Bay (type locality) [27], Xiamen Harbour [48], Bay of Bengal [43] and Muscat Oman [9]. Gu and co-authors found [48] *S. grevillei* in Xiamen Harbour from August to September, but they do not report on abundances or any other ecological factors accompanying the bloom. As *S. grevillei*

appeared in the warm season in Xiamen Harbour, and in the Arabian Sea as well [9], the authors suggested that this is a tropical species that occurs also in the warm season of warm temperate regions [48] and is characterised as summer/autumn species. But there is only a limited number (seven in total) of publications mentioning this species, and so far, none of them reporting on ecology. We observed larger abundances during the autumn bloom shortly after the onset of water column mixing in September and December, when water temperatures started dropping more rapidly. Water temperature in samples containing *S. grevillei* ranged from 10.06 to 21.79 °C with a median of 16.08 °C. Highest abundances for *S. grevillei* were observed along the eastern Adriatic coast and specifically in harbour bays (Fig. 5) which is in strong contrast with the preference of *S. marinoi*, which appears to prefer nutrient-loaded open waters closer to the River Po mouth (Fig. 4). *S. grevillei* thrives in elevated nutrient concentrations but appears to prefer higher salinities (see Fig. 6). Figure 6 demonstrates a nonsignificant trend of elevated nutrient salt concentrations during *S. marinoi* observations. This might be explained by *S. marinoi*'s capability to outcompete other diatom species during bloom conditions, while *S. grevillei* under such competitive conditions rather vanishes. This probably indicates that its tolerance towards reduced salinity is not as pronounced as it is for *S. marinoi* [49].

S. menzelii appears regularly in small abundances during winter months (December–January). It is more prominent along the eastern Adriatic coast where the phytoplankton abundances are lower and biodiversity is higher. However, *S. menzelii* never dominates the microphytoplankton community and is observed rather sporadically. It reaches abundances of up to 5680 cells L^{-1}. Given the low frequency and only sporadic observations at this time, we cannot extract significant correlations between ecological parameters and the abundances of *S. menzelii*. It is well possible that *S. menzelii* is not establishing a permanent population in the Northern Adriatic, but its presence is rather due to advection with water masses from the middle and southern Adriatic.

Genetic Analysis

Both analysed genetic markers for *S. marinoi* were identical to previously published sequences of isolates from other regions. This supported the unequivocal taxonomic identification of *S. marinoi* as such. This result indicates furthermore that the Northern Adriatic *S. marinoi* probably is part of a globally distributed and possibly connected population. This observation is in accordance to the finding of Kooistra and colleagues [50]. *S. grevillei* on the other hand for both marker regions showed marked sequence differences from earlier published sequences for isolates from different locations (see Supplementary Fig. 2). Supplementary Fig. 4 shows the genetic distances within the D1–D3 region of the LSU rDNA for all analysed sequences. Most similar sequences are reported for isolates from the coastal water off Yemen and off Japan. Sequences that are more dissimilar are reported for isolates from the coastal waters off India and China. This observation cannot be explained by ocean currents. Natural genetic drift over or along communicating populations and geographic distances would result in a unidirectional gradient of genetic distance. In this case, however, it rather appears that there is a shortcut from Japan waters to the Adriatic that might include the coastal water off Yemen. Ballast water transport from Japan through the Red Sea and the Suez Channel into the Adriatic would explain the genetic similarity of Adriatic isolates with isolates from the coast off Yemen at the southern entrance into the red sea and with isolates from Japan.

S. menzelii was only observed sporadically, and no cell culture was established for subsequent genetic analysis.

Summary

We observed three species from the genus *Skeletonema* in the northern Adriatic: *S. marinoi*, *S. grevillei* and *S. menzelii*.

S. marinoi appears throughout large parts of the year with expressed blooms in late winter and early spring when water temperatures are low and nutrient concentrations are high. *S. marinoi* dominates highly productive microphytoplankton blooms in coastal and open waters and appears generally well adapted to steep spatiotemporal ecological gradients as present in the northern Adriatic [51, 52]. Genetic similarity to most sequences from available isolates from other marine areas suggests a large and interconnected population structure with mechanisms for conservation of genetic markers.

S. grevillei is observed in autumn and early winter, when temperatures fall and nutrients become available through water column mixing. Like *S. marinoi*, it appears to be a stable constituent of the northern Adriatic phytoplankton. However, the species never dominates the phytoplankton community. Highest abundances were observed in harbour bays and along the eastern Adriatic coast. Clearly, *S. grevillei* prefers higher nutrient concentrations and harbour areas. Its preference for coastal proximity and inability to dominate massive bloom events might explain a slower distribution rate across large distances and a generally higher genetic variability between isolated geographically distant locations. It also might make *S. grevillei* a successful traveller in ballast waters. It certainly appears that the *S. grevillei* population we observed in the northern Adriatic might be a permanently introduced species to the area.

S. menzelii was observed only sporadically and with low abundances in the northern Adriatic. It probably is not a permanent constituent of the northern Adriatic, but rather appears when advected from more southern parts of the Adriatic,

where temperature is more stable and generally higher and where nutrient concentrations are lower and less fluctuating.

Acknowledgements We are grateful for the work of Jasna Jakovcevic, Denis Skalic and Margareta Buterer in ocean sampling and in the analysis of oceanographic parameters as well as in database handling. This work was supported by the Ministry of Science, Education and Sports of the Republic of Croatia as well as by the scientific project UIP-2014-09-6563 (Phytoplankton life strategies in the northern Adriatic), funded by the Croatian Science Foundation as well as by the EU SYNTHESYS projects DE-TAF-4090 and DE-TAF-4112. D.M.P. is grateful to teachers and colleagues from the 11th Advanced Phytoplankton Course where these results were discussed for the first time. We are grateful to two anonymous reviewers for their insightful improvements of the manuscript.

References

1. Falkowski PG, Barber RT, Smetacek V (1998) Biogeochemical controls and feedbacks on ocean primary production. Science 281:200–206
2. Buchan A, LeCleir GR, Gulvik CA, Gonzalez JM (2014) Master recyclers: features and functions of bacteria associated with phytoplankton blooms. Nat Rev Microbiol 12:686–698. https://doi.org/10.1038/nrmicro3326
3. Round FE, Crawford RM, Mann DG (1990) The diatoms. Biology and morphology of the genera. Cambridge University Press, Cambridge,
4. Cloern JE, Cole BE, Wong RLJ, Alpine AE (1985) Temporal dynamics of estuarine phytoplankton: a case study of San Francisco Bay. Hydrobiologia 129:153–176
5. Estrada M, Vives F, Alcaraz M (1985) Life and the productivity of the open sea. In: Margalef R (ed) Western Mediterranean. Pergamon Press, pp. 148–197
6. Cleve PT (1900) Notes on some Atlantic plankton-organisms. Konglica Svenska Vetenskaps-Akademiens Handlingar 34:3–22
7. Hasle GR (1973) Morphology and taxonomy of *Skeletonema costatum* (Bacillariophyceae). Nor J Bot 20:109–137
8. Karentz D, Smayda TJ (1984) Temperature and seasonal occurrence patterns of 30 dominant phytoplankton species in Narragansett Bay over a 22-year period (1959-1980). Mar Ecol Prog Ser 18:277–293
9. Kooistra WCHF, Sarno D, Balzano S, Gu H, Andersen RA, Zingone A (2008) Global diversity and biogeography of *Skeletonema* species (Bacillariophyta). Protist 159:177–193
10. Greville RK (1865) Description of new and rare diatoms. Series 16. Transactions of the Microscopical Society of London, New Series 13:43–57
11. Shevchenko OG, Ponomareva AA (2015) The morphology and ecology of the marine diatom *Skeletonema marinoi* Sarno et Zingone, 2005 from the Sea of Japan. Russ J Mar Biol 41:490–494. https://doi.org/10.1134/S1063074015060127
12. Sarno D, Kooistra WCHF, Medlin LK, Percopo I, Zingone A (2005) Diversity in the genus *Skeletonema* (Bacillariophyceae). II. An assessment of the taxonomy of *S. costatum*-like species, with the description of four new species. J Phycol 41:151–176
13. Guiry MD, Guiry DM (2017) AlgaeBase. World-wide electronic publication, National University of Ireland, Galway. http://www.algaebase.org. Accessed 18 July 2017
14. Hevia-Orube J, Orive E, David H, Laza-Martinez A, Seoane S (2016) *Skeletonema* species in a temperate estuary: a morphological, molecular and physiological approach. Diatom Res 31:185–197. https://doi.org/10.1080/0269249X.2016.1228548
15. Ivančić I, Degobbis D (1987) Mechanisms of production and fate of organic phosphorus in the northern Adriatic Sea. Mar Biol 94:117–125
16. Harding LWJ, Degobbis DRP (1999) Production and fate of phytoplankton: annual cycles and interannual variability. In: Malone TC, Malej A, Harding Jr LW, Smodlaka N, Turner RE (eds) Ecosystem at the land-sea margin: drainage basin to coastal sea. American Geophysical Union, Washington, DC, pp. 131–172
17. Degobbis D, Precali R, Ivancic I, Smodlaka N, Fuks D, Kveder S (2000) Long-term changes in the northern Adriatic ecosystem related to anthropogenic eutrophication. Int J Environ Pollut 13:495–533
18. Russo A, Maccaferri S, Djakovac T, Precali R, Degobbis D, Deserti M, Paschini E, Lyons DM (2005) Meteorological and oceanographic conditions in the northern Adriatic Sea during the period June 1999–July 2002: influence on the mucilage phenomenon. Sci Total Environ 353:24–38. https://doi.org/10.1016/j.scitotenv.2005.09.058
19. Ivančić I, Godrijan J, Pfannkuchen M, Marić D, Gašparović B, Djakovac T, Najdek M (2012) Survival mechanisms of phytoplankton in conditions of stratification-induced deprivation of orthophosphate: northern Adriatic case study. Limnol Oceanogr 57. https://doi.org/10.4319/lo.2012.57.6.0000
20. Ivančić I, Pfannkuchen M, Godrijan J, Djakovac T, Marić Pfannkuchen D, Korlević M, Gašparović B, Najdek M (2016) Alkaline phosphatase activity related to phosphorus stress of microphytoplankton in different trophic conditions. Prog Oceanogr 146:175–186. https://doi.org/10.1016/j.pocean.2016.07.003
21. Marić D, Kraus R, Godrijan J, Supić N, Djakovac T, Precali R (2012) Phytoplankton response to climatic and anthropogenic influences in the north-eastern Adriatic during the last four decades. Estuar Coast Shelf Sci. https://doi.org/10.1016/j.ecss.2012.02.003
22. Parsons TR, Maita Y, Lalli CM (1984) A manual of chemical and biological methods for seawater analysis. Pergamon Press, Toronto,
23. Ivančič I, Degobbis D (1984) An optimal manual procedure for ammonia analysis in natural waters by the indophenol blue method. Water Res 18:1143–1147. https://doi.org/10.1016/0043-1354(84)90230-6
24. Mikulic N, Degobbis D, Picer M, Raspor B, Sipos L, Sobot S, Zvonaric T, Precali R (1994) UNEP: monitoring programme of the eastern adriatic coastal area. United Nations Environment Programme. Report for 1983–1991. MAP Technical Report Series No. 86. Athens, pp. 316
25. Hasle GR (1978) Diatoms. In: Sournia A (ed) Phytoplankton manual. UNESCO, Paris, France, pp. 136–142
26. Utermöhl H (1958) Zur Vervollkommnung der quantitativen Phytoplankton-Methodik. Mitteilungen der Internationale Vereinigung für theoretische und angewandte Limnologie, vol 9. Schweizerbart, Stuttgart, pp. 1–38
27. Zingone A, Percopo I, Sims PA, Sarno D (2005) Diversity in the genus *Skeletonema* (Bacillariophyceae). I. A re-examination of the type material of *Skeletonema costatum*, with the description of *S. grevillei* sp. nov. J Phycol 41:140–150
28. Guillard RRL (1975) Culture of phytoplankton for feeding marine invertebrates. In: Smith WL, Chanley MH (eds) Culture of marine invertebrate animals. Plenum Press, New York, pp. 29–60
29. Anonymous (1975) Proposals for a standardization of diatom terminology and diagnoses. Nova Hedwig Beih 53:323–354
30. Ross R, Cox EJ, Karayeva NI, Mann DG, Paddock TBB, Simonsen R, Sims PA (1979) An amended terminology for the siliceous components of the diatom cell. Nova Hedwig Beih 64:513–533
31. Zimmermann J, Jahn R, Gemeinholzer B (2011) Barcoding diatoms: evaluation of the V4 subregion on the 18S rRNA gene, including new primers and protocols. Org Divers Evol 11:173–192. https://doi.org/10.1007/s13127-011-0050-6

JrnlID 248_ArtID 1069_Proof# 1 - 12/09/2017

32. Orsini L, Sarno D, Procaccini G, Poletti R, Dahlmann J, Montresor M (2002) Toxic *Pseudo-nitzschia multistriata* (Bacillariophyceae) from the Gulf of Naples: morphology, toxin analysis and phylogenetic relationships with other *Pseudo-nitzschia* species. Eur J Phycol 37:247–257
33. Pruesse E, Quast C, Knittel K, Fuchs BM, Ludwig W, Peplies J, Glockner FO (2007) SILVA: a comprehensive online resource for quality checked and aligned ribosomal RNA sequence data compatible with ARB. Nucleic Acids Res 35:1–9. https://doi.org/10.1093/nar/gkm864
34. Ludwig W, Strunk O, Westram R, Richter L, Meier H, Yadhukumar BA, Lai T, Steppi S, Jobb G, Förster W, Brettske I, Gerber S, Ginhart AW, Gross O, Grumann S, Hermann S, Jost R, König A, Liss T, Lüßmann R, May M, Nonhoff B, Reichel B, Strehlow R, Stamatakis A, Stuckmann N, Vilbig A, Lenke M, Ludwig T, Bode A, Schleifer K-H (2004) ARB: a software environment for sequence data. Nucleic Acids Res 32:1363–1371
35. Peplies J, Kottmann R, Ludwig W, Glöckner FO (2008) A standard operating procedure for phylogenetic inference (SOPPI) using (rRNA) marker genes. Syst Appl Microbiol 31:251–257
36. R_Core_Team (2015) R: A language and environment for statistical computing. R Foundation for Statistical Computing
37. Harrell FE (2017) Hmisc: Harrell Miscellaneous
38. Team RC (2015) R: a language and environment for statistical computing
39. Wickham H (2009) ggplot2: elegant graphics for data analysis. Springer-Verlag, New York,
40. Peterson BG, Carl P (2014) PerformanceAnalytics: econometric tools for performance and risk analysis. R package version 0.9
41. Fisher RA (1926) The arrangement of Fiels Experiements. J Min Agric Great Britain 33:503–513
42. Sarno D, Kooistra WCHF, Balzano S, Hargraves PE, Zingone A (2007) Diversity in the genus *Skeletonema* (Bacillariophyceae): III. Phylogenetic position and morphological variability of *Skeletonema costatum* and *Skeletonema grevillei*, with the description of *Skeletonema ardens* sp. nov. J Phycol 43:156–170
43. Naik RK, Sarno D, Kooistra WHCF, D'Costa PM, Anil AC (2010) Skeletonema (Bacillariophyceae) in Indian waters: a reappraisal. Indian J Mar Sci 39:290–293
44. Guillard RRL, Carpenter EJ, Reimann BEF (1974) Skeletonema menzelii sp. nov., a new diatom from the western Atlantic Ocean. Phycologia 13:131–138. https://doi.org/10.2216/i0031-8884-13-2-131.1
45. Yamada M, Katsuki E, Otsubo M, Kawaguchi M, Ichimi K, Kaeriyama H, Tada K, Harrison PJ (2010) Species diversity of the genus *Skeletonema* (Bacillariophyceae) in the industrial harbor Dokai Bay, Japan. J Oceanogr 66:755–771. https://doi.org/10.1007/s10872-010-0062-4
46. Guillard RRL, Carpenter EJ, Reimann BEF (1974) *Skeletonema menzelii* sp. nov., a new diatom from the western Atlantic Ocean. Phycologia 13:131–138
47. Ribera d'Alcalà M, Conversano F, Corato F, Licandro P, Mangoni O, Marino D, Mazzocchi MG, Modigh M, Montresor M, Nardella M, Saggiomo V, Sarno D, Zingone A (2004) Seasonal patterns in plankton communities in a pluriannual time series at a coastal Mediterranean site (Gulf of Naples): an attempt to discern recurrences and trends. Sci Mar 68(Suppl. 1):65–83
48. Gu H, Zhang X, Sun J, Luo Z (2012) Diversity and seasonal occurrence of Skeletonema (Bacillariophyta) species in Xiamen Harbour and surrounding seas, China. Cryptogam Algol 33:245–263
49. Balzano S, Sarno D, Kooistra WHCF (2011) Effects of salinity on the growth rate and morphology of ten Skeletonema strains. J Plankton Res 33:937–945. https://doi.org/10.1093/plankt/fbq150
50. Kooistra WCHF, Sarno D, Balzano S, Gu H, Andersen RA, Zingone A (2008) Global diversity and biogeography of Skeletonema species (Bacillariophyta). Protist 159:177–193
51. Godrijan J, Marić D, Tomažić I, Precali R, Pfannkuchen M (2013) Seasonal phytoplankton dynamics in the coastal waters of the northeastern Adriatic Sea. J Sea Res 77:32–44. https://doi.org/10.1016/j.seares.2012.09.009
52. Maric D, Frka S, Godrijan J, Tomazic I, Penezic A, Djakovac T, Vojvodic V, Precali R, Gasparovic B (2013) Organic matter production during late summer-winter period in a temperate sea. Cont Shelf Res 55:52–65. https://doi.org/10.1016/J.Csr.2013.01.008

AUTHOR QUERIES

AUTHOR PLEASE ANSWER ALL QUERIES.

Q1. Kindly check the names of authors if correctly captured and presented.
Q2. Kindly check if the table entries, notes, and other relevant details (Tables 1 to 3) are correctly captured and presented
Q3. Figures were renumbered (orginally, Figs. 1 to 7, 10 and 8). Please check.
Q4. Missing Fig. 10 citation is inserted here. Please check.
Q5. Please check inserted suggested captions for Figs. 9 and 10 if appropriate; otherwise, kindly provide more suitable ones.
Q6. Please advise if the captured abbreviated journal title is correct.